Fluorescent Molecularly Imprinted Nanogels for the Detection of Anticancer Drugs in Human Plasma

Elena Pellizzoni[a,b], Martina Tommasini[a], Elena Marangon[c], Flavio Rizzolio[c], Gabriele Saito[d] Fabio Benedetti[a], Giuseppe Toffoli[c,]*, Marina Resmini[d,]*, Federico Berti[a,]*.

[a]: Dipartimento di Scienze Chimiche e Farmaceutiche, Università degli Studi di Trieste, Italy (elena.pellizzoni@phd.units.it, martina.tommasini@phd.units.it, benedett@units.it, fberti@units.it)

[b]: Graduate School of Nanotechnology, Università degli Studi di Trieste, Italy

[c]: CRO National Cancer Institute Experimental and Clinical Pharmacology Division, Department of Translational Research, Aviano, Italy (frizzolio@cro.it, emarangon@cro.it, gtoffoli@cro.it)

[d]: Department of Chemistry and Biochemistry, SBCS, Queen Mary University of London, UK (g.saito@qmul.ac.uk, m.resmini@qmul.ac.uk)

*Giuseppe Toffoli, Centro di Riferimento Oncologico, IRCCS, Via Franco Gallini 2, 33081 Aviano, Italy, +39 0434 659235, gtoffoli@cro.it; Federico Berti, Dipartimento di Scienze Chimiche e Farmaceutiche, via Giorgieri 1, 34128 Trieste, Italy, +39 040 5583920, fberti@units.it; Marina Resmini, Department of Chemistry and Biochemistry, SBCS, Queen Mary University of London, Mile End Road, London E1 4NS, UK +44 (0)20 78823268, m.resmini@qmul.ac.uk.

Abstract

Several fluorescent molecularly imprinted nanogels for the detection of the anticancer drug sunitinib were synthesized and characterised. A selection of functional monomers based on different aminoacids and coumarin allowed isolation of polymers with very good rebinding properties and sensitivities. The direct detection of sunitinib in human plasma was successfully demonstrated by fluorescence quenching of the coumarin-based nanogels. The plasma sample simply diluted in DMSO allowed the recovery of various amounts of sunitib, as determined by an averaged calibration curve. The LOD was 400 nM, with within-run variability < 9%, day to day variability < 5%, and good accuracy in the recovery of sunitinib from spiked samples.

Keywords: therapeutic drug monitoring, anticancer drugs, imprinted polymers, human plasma, fluorimetry.

1. Introduction

Keeping toxicity to a minimal level while ensuring optimal activity and minimal side effects are key priorities in cancer therapy, however, individual germ line mutations, in metabolizing enzymes, and other pharmacogenomics variations may vary pharmacokinetic and pharmacodynamic responses within a pool of individuals. Therapeutic drug monitoring, aimed at obtaining personalized medicines, is one of the main targets in current clinical oncology (Walko and McLeod 2014; De Jonge at al. 2005; Alnaim 2007). At present, therapeutic drug monitoring (TDM) heavily relies on drug extraction and quantification from blood or plasma samples by HPLC (Mohammadi et al. 2010) or LC-MS (Marangon et al. 2015; Van Erp et al. 2013). The instrumentation required for these analyses is expensive and dependent on highly specialised personnel, therefore limiting the applicability. The development of a point of care device, that allows tailoring of the therapy protocol upon individual responses, with simple sample preparation, high sensitivity and good selectivity, remains a challenge.

In recent years molecular imprinting has consolidated its place as a viable approach for the generation of polymeric matrices with excellent molecular recognition characteristics. The templating approach, together with an appropriate choice of functional monomer and cross-linker, allows the formation of three-dimensional cavities that can rebind the target molecule, or its analogues, with high selectivity.

In the field of therapeutic drug monitoring, imprinted polymers (MIPs) have been developed for pre-concentration of samples, as purification cartridges for LC-MS analysis (Thibert et al. 2014; Yang et al. 2014), or as recognition elements for microbalances, plasmon resonance and electrochemical systems (Altintas et al. 2015; Blanco-Lòpez et al. 2004). Alternatively, MIPs have also been used as the sensing system, by embedding the signal-generating monomer in the polymeric matrix, such as in the case of optical/fluorimetric units (Manju et al. 2010; Awino and Zhao 2014; Ton et al. 2013). In terms of polymer matrices, most work has been done with bulk polymers, acting as recognition elements for electrochemical, quantum dots or fiber optic based sensors. MIP-based electrochemical sensors have been used to detect uracil- (Prasad et al. 2012; Prasad et al. 2009) and anthraquinone-based anticancer drugs (Nezhadali et al. 2016). CdTe@SiO_2 quantum dots coated with a MIP were used as fluorescent sensor for norepinephrine (Wei et al. 2014), and fiber optic array was developed to quantify enrofloxacin in sheep serum (Carrasco et al. 2015).

The main target of this work was to develop fluorescent imprinted nanogels, specific for anticancer drugs, that would form stable colloidal solutions when dispersed into human plasma, therefore allowing detection of the target with minimal sample preparation.

Plasma is a very complex matrix, containing thousands of different molecules and binding proteins such as albumins and immunoglobulins. A potential sensor for the quantification of drugs must overcome key issues like the possible cross-reactivity with plasma proteins and

small molecules, competitive binding of the drug to albumin, stability issues leading to aggregation and precipitation of the nanoparticles.

For the purpose of this work sunitinib (SU11248, Sutent) **1 (Figure 1)** was selected as the target drug. Sunitinib is a tyrosine kinase inhibitor used for the treatment of renal cell carcinoma and of imatinib-resistant gastrointestinal stromal tumour since 2006 (Noble et al. 2004; Zhang et al. 2009). It is commonly administered to patients as sunitinib malate, with dosages ranging from 25-50 mg to 150 mg daily. Pharmacokinetic and pharmacodynamic preclinical studies demonstrated that although the therapeutic window of concentrations for sunitinib is between 50 ng/mL and 500 ng/mL, concentrations higher than 100 ng/mL result in a significant increase in drug toxicity (Faivre et al. 2006; Kollmannsberger et al. 2011). Therefore, the TDM of this drug represents a useful system to develop personalized therapies for patients decreasing side effects and increasing therapy efficiency. As for other anticancer drugs, sunitinib quantification in plasma is currently performed by HPLC coupled with UV detector (Etienne-Grimaldi et al. 2009; Blanchet et al. 2009) or mass spectrometer (De Bruijn et al. 2010) or by LC/MS/MS methods (Andriamanana et al. 2013). Currently there are no rapid methods available for the therapeutic monitoring of sunitinib in alternative to such high specialised equipment, and point of care devices or immunoenzymatic assays for anticancer drugs have yet to be reported.

2. Materials and Methods

***Materials*:** Sunitinib was purchased from Bepharm ltd. All the other reagents were from Sigma-Aldrich.

Instrumentation*:* HPLC analyses were run on an *Agilent series 1100* liquid chromatograph equipped with a *Phenomenex*, *Luna C18* 5μ column with a column guard and a 20 μL loop. The flow was set to 1 mL min^{-1}. UV-visible spectra were recorded on a *UV-1800 (Shimadzu)* spectrometer. The fluorescence titrations were performed by a *CARY Eclipse (Varian)* spectrometer with a cuvette of 1 cm optical path, and by a *Perkin Elmer LS 50B* fluorescence

spectrometer. Nuclear magnetic resonance spectra (500 MHz) were recorded on a *Varian 500* spectrometer. Polymeric particles were analysed by Dynamic Laser Light Scattering on a *Zetasizer nano-S (Malvern)* instrument.

Methyl 2-acrylamido-3-(4-hydroxyphenyl)propanoate (*N*-acryloyl L-tyrosine methyl ester **3b**): acryloyl chloride (1 mL, 12.3 mmol) in 50 mL anhydrous dichlorometane (DCM) was added dropwise, at 0 °C, to a solution of triethylamine (4.5 mL, 32.4 mmol) and L-tyrosine methyl ester (2 g, 10.2 mmol) in 150 mL DCM and the reaction mixture was stirred overnight under anhydrous atmosphere. The solvent was removed *in vacuo* and the crude product was purified by silica gel column chromatography (DCM:ethyl acetate from 1:1 to 2.5:7.5) giving the product **3b** (1.2 g, 47%). White crystals, **mp**: 125.6 – 129 °C. **^{1}H NMR** (500 MHz, $CDCl_3$, 25°C) δ = 3.05 (dd, ^{2}J = 14 Hz, ^{3}J = 9 Hz, 1H), 3.12 (dd, ^{2}J = 14 Hz, ^{3}J = 6 Hz, 1H), 3.75 (s, 3H), 4.94 (m, 1H), 4.68 (dd, $^{3}J_{trans}$ = 10 Hz, $^{3}J_{cis}$ = 1.2 Hz, 1H), 5.93 (s, 1H), 6.10 (br), 6.09 (dd, ^{2}J = 17 Hz, $^{3}J_{trans}$ = 10 Hz), 6.29 (dd, $^{2}J_{trans}$ = 17 Hz, $^{3}J_{cis}$ = 1.2 Hz), 6.73 (d, ^{3}J = 8.5 Hz, 2H), 6.94 (d, ^{3}J = 8.5 Hz, 2H). **^{13}C NMR** (500 MHz, $CDCl_3$, 25°C) δ = 37.27, 52.62, 53.49, 115.69, 127.41, 127.70, 130.30, 130.51, 152.32, 165.30, 172.27. **MS (ESI)** *m/z*: 272.0 $[M+Na]^{+}$; **IR**: ν cm^{-1} = 1662, 1721 cm^{-1}, 3318.

(S)-methyl 2-acrylamido-3-(1H-indol-3-yl)propanoate (*N*-acryloyl L-tryptophan methyl ester **4b**): acryloyl chloride (0.2 mL, 2.3 mmol) in 5 mL DCM was added dropwise, at 0 °C, to a solution of L-tryptophan methyl ester (0.5 g, 1.96 mmol) and triethylamine (0.67 mL, 4.8 mmol) in 10 mL anhydrous DCM and the reaction mixture was stirred overnight under anhydrous atmosphere. The solvent was removed *in vacuo* and the crude product was purified by silica gel column chromatography (DCM:ethyl acetate from 8:2 to 5:5) giving the product **4b** (0.4 g, 81%). White crystals, **mp**: 49-49.5 °C. **^{1}H-NMR** (500 MHz, d_6-DMSO, 25°C) δ = 3.07 (dd, ^{2}J = 14.6 Hz, ^{3}J = 8.5 Hz), 3.18 (dd, ^{2}J = 14.6 Hz, ^{3}J = 5 Hz), 3.59 (s, 3H), 4.60 (m, 1H), 5.60 (dd, $^{3}J_{cis}$ = 2 Hz, $^{3}J_{trans}$ = 10 Hz), 6.07 (dd, ^{2}J = 17.11 Hz, $^{3}J_{cis}$ = 2 Hz), 6.29 (dd, ^{2}J = 17.11 Hz,

$^3J_{trans}$ = 10Hz, 1H), 6.98 (td, $^3J_{ortho}$ = 8 Hz, $^4J_{meta}$ = 1 Hz, 1H), 7.06 (td, $^4J_{meta}$ = 1 Hz, $^3J_{ortho}$ = 4 Hz, 1H), 7.13 (d, ^3J = 2 Hz, 1H), 7.33 (d, $^3J_{ortho}$ = 8 Hz, 1H), 7.49 (d, $^3J_{ortho}$ = 8 Hz, 1H), 8.54 (d, ^3J = 8 Hz, 1H), 10.85 (s, 1H). **^{13}C-NMR** (500 MHz, d_6-DMSO, 25°C) δ = 27.79, 52.55, 53.21, 110.14, 111.41, 118.76, 119.89, 122.41, 122.90, 127.29, 127.82, 130.56, 136.33, 165.13, 172.38. **MS** ESI *m/z*: 295 $[M+Na]^+$; **IR**: ν cm^{-1}= 1662, 1737, 3296.

2-oxo-2H-chromen-7-yl acrylate (7-O-acryloyl-hydroxycoumarin **5b**): acryloyl chloride (0.4 mL, 4.6 mmol) in 7 mL DCM was added dropwise, at 0 °C, to a solution of 7-hydroxy-coumarin (0.5 g, 3.08 mmol) and triethylamine (1.26 mL, 9.06 mmol) in 10mL anhydrous DCM and the reaction mixture was stirred overnight under anhydrous atmosphere. The reaction mixture was extracted with brine, filtered and extracted 3 more times with brine. The organic phase was evaporated *in vacuo* and the orange residue was purified by flash chromatography (DCM : petroleum ether:ethyl acetate 2:1:1) to yield pure **5b** (0.6 g, 90%). White crystals, **mp**: 136.9-137.5 °C. **^{1}H-NMR** (500 MHz, $CDCl_3$, 25°C) δ = 6.08 (dd, $^3J_{trans}$ = 10.5 Hz, $^3J_{cis}$ = 1 Hz, 1H), 6.33 (dd, $^3J_{trans}$ = 10.5 Hz, ^2J= 17 Hz, 1H), 6.40 (d, $^3J_{ortho}$ = 9.6 Hz, 1H), 6.65 (dd, ^2J = 17 Hz, $^3J_{cis}$ = 1 Hz, 1H), 7.10 (dd, $^3J_{ortho}$ = 8.4 Hz, $^4J_{meta}$ = 2 Hz, 1H), 7.17 (d, $^4J_{meta}$ = 2 Hz, 1H), 7.50 (d, $^3J_{ortho}$ = 8.4 Hz, 1H), 7.70 (d, $^3J_{ortho}$ = 9.6 Hz, 1H). **^{13}C-NMR** (500 MHz, $CDCl_3$, 25°C) δ = 110.57, 116.27, 116.86, 118.49, 127.44, 128.70, 133.82, 142.96, 153.23, 154.85, 160.45, 163.90. **MS** ESI *m/z*: 238.9 $[M+Na]^+$; **IR**: ν cm^{-1} = 1734.

^{1}H NMR titrations

Weighted amounts of functional monomer **3b**, **4b**, **5b** were added to a 6.7 mM solution of sunitinib in DMSO-d_6 so that the concentration of functional monomer varied from 3.35 mM to 93.7 mM. Sunitinib (6.7 mM) was also titrated with 4-vinylpyridine (**2**) using a 1.15 M mother solution in DMSO-d_6. The ^{1}H NMR spectrum of the resulting solutions were recorded after every addition. (**Figure 1**).

Synthesis of molecularly imprinted polymers (general procedure)

The functional monomer (1 equiv) and the template drug (1.2 equiv) were stirred in DMSO, in anhydrous conditions, for 40 minutes. The resulting solution was transferred in a crimp cap Wheaton vial and *N,N'*-ethylenebisacrylamide (crosslinker, 4.7 equiv), recrystallized[1] AIBN (18% mol, calculated on the amount of the available double bonds, 2.1 equiv) and acrylamide (1equiv) were added. DMSO was adjusted so as to correspond to 99% of total monomers and crosslinker (in weight) and the vial was evacuated, flushed with argon (3 x 10 minutes) and then kept at 70°C for 4 days. Each polymer was synthesised both in presence of the template molecule, leading to MIP particles, and without the template, leading to NIP (non-imprinted polymers). The resulting clear solutions were dialyzed (cut off 3.5 kDa) against methanol for 2 days and against water for other 2 days, changing the solvent 3 times per day. Finally, the solutions were freeze-dried giving a fluffy solid. The composition and quantities of the polymerization mixtures for each nanogels are reported in **Table S1**. The solid polymers were reconstituted at the desired concentration by dispersing the nanogels in the required solvent, sonnication for 10 minutes and filtration using Micron filter (0.25μm pore size).

Dynamic laser light scattering

Characterisation of particle size was done in the same solvent system that was used for the rebinding assays in plasma. The size distribution by number, intensity and by volume was recorded in triplicate for solutions of all MIPs and NIPs (0.25 mg mL^{-1}, 10% H_2O in DMSO).

Transmission electron microscopy

MIP 1.4 (1.08 mg) was dissolved in 2.16 mL of distilled water, the solution was stirred for 10 minutes and sonicated for 15 minutes. The resulting solution was dialyzed for 24 h at 25°C in distilled water using a pre-wetted Float-A-Lyzer® G2 with MWCO = 3.5 - 5.0 kDa (obtained

[1] 2 g of AIBN were placed in a round-bottomed flask equipped with a stirring bar and a condenser. The flask was evacuated and purged with argon for 10 times, to avoid any trace of oxygen. 5 mL of degassed ethanol were added and the temperature was increased slowly to 50-55 °C. 2 mL of ethanol were added to solubilize the product and the flask was then left to cool to room temperature to allow crystallization.

by Spectrumlabs). The solution was then filtered through a 0.45 μm GHP membrane and a 2.0 μl were added to graphene oxide grid (GO support film on Lacey carbon on 400 mesh Cu grid, Agar Scientific) and imaged at TEM.

Rebinding tests of the drug

A mixture of polymer (1.5 mg) and the drug (50 μM) in 1.5 mL water was incubated at 25°C with continuous stirring; 200 μL aliquots were taken after 1 h, 3 h, 8 h and spiked with 50 μL of a 1 μM solution of a reference standard. Each aliquot was centrifuged (10000 rpm for 6 min) and the supernatant, containing an unknown amount of the drug and 25 μM reference, was analysed by HPLC to quantify the drug concentration. The reference standard for sunitinib was caffeic acid and the mobile phase was 75 : 25 water : acetonitrile with 0.05% of TFA, wavelength: 265 nm.

Cross reactivity tests with SN38 and paclitaxel were performed in the same manner with 50 μM SN38 or paclitaxel in water, using 25 μM quinolinone as reference. SN38 was analysed with 78 : 22 water : acetonitrile mixture containing 0.05% TFA as the mobile phase, a flux of 1 mL/min and the detector fixed at 208 nm wavelength. For paclitaxel, 55 : 45 water : acetonitrile containing 0.05% TFA was used as the mobile phase with a flux of 1 mL/min, and the wavelength was set at 230 nm.

Fluorimetric characterization of the polymers

The fluorescence of 60 μg/mL solutions of the fluorescent polymers in water containing 3% DMSO and sunitinb ranging from 0 to 88.8 μM was measured at the following wavelengths: 303 nm (emission) and 274 nm (excitation) for polymers containing tyrosine; 340 nm (emission) and 280 nm (excitation) for polymers containing tryptophan; 456 nm (emission) and 327 nm (excitation) for polymers containig coumarin. The fluorescence of solutions of the corresponding fluorophores, namely 2.1 μM *N*-Boc-tyrosine, 510 nM *N*-Boc-tryptophan, and

5 μM 7-hydroxy-coumarin, were similarly measured in the presence of sunitinib ranging from 0 to 73 μM.

Fluorescence assay in plasma

Calibration curve. A 1.0 mg/mL solution of MIP **1.5** in DMSO was diluted to a final 60 μg/mL concentration in 4 : 1 DMSO : water. In order to obtain the calibration curve, 400 μL of this solution were titrated with increasing amounts of 400 μM and 4 mM sunitinib solutions in 4 : 1 DMSO-water so that the final sunitinib concentration was in the 1 μM -154 μM range.

Spiked samples. The spiked samples at 5 μM, 20 μM, 50 μM and 80 μM sunitinib were made diluting a 4 mM sunitinib solution with 50 mg/mL HSA in PBS or with plasma to the required concentrations. DMSO (400 μL) was added to 100 μL of this solution and the mixture was centrifuged. MIP was added to the supernatant so that the final polymer concentration was 60 μg/mL and the fluorescence of the solution was measured at the following wavelengths: 456 nm (emission) and 327 nm (excitation) with bandwidths set at 5 nm.

3. Results and discussion

Functional monomers

The formation of a stable complex between the functional monomer and the template in the prepolymerisation mixture is a key requirement in molecular imprinting for obtaining matrices with high rebinding characteristics. Four functional monomers were selected for their potential ability to interact with Sunitinib, the target drug, via a variety of non-covalent interactions. Sunitinib (**Figure 1**) contains three hydrogen bond donor NH groups, three hydrogen bond acceptors (two carbonyls and a tertiary amino group), an extended aromatic system capable of π-staking, and four alkyl sites candidates for van der Waals and hydrophobic interactions. 4-Vinyl pyridine **2** is a functional monomer that may interact by π-π stacking and hydrogen bonds to the nitrogen atom and has been chosen as a reference monomer, being commercially

available. N-acryloyl-tyrosine methyl ester **3b** and N-acryloyl-tryptophan methyl ester **4b** were selected to exploit biomimetic recognition of the targets by the amino acid side chains. In addition, tryptophan has the advantage of being fluorescent with an emission at 340 nm (excitation at 280 nm). The static quenching of this fluorescence by many interacting molecules is often exploited in studies of protein-small molecule interactions (Luisi et al. 2013). 7-Acryloyloxy-coumarin **5b** contains the coumarin fluorophore that emits visible light at 460 nm upon excitation at 330 nm: this feature, and its molecular structure, potentially capable of establishing π-π stacking interactions with the aromatic regions of Sunitinib, may lead to a light-emitting sensor that can be switched off when binding the target.

Compounds **3b**, **4b, 5b** were obtained by acylation of the corresponding precursors **3a-5a** with acryloyl chloride following previously reported procedures (Bentolila et al. 2000; Moore and O'Relly 2012; Sinkel et al. 2010).

In order to assess whether compounds **3b-5b** can establish strong interactions with the target, a series of ^{1}H-NMR titrations were performed in DMSO by adding different concentrations of functional monomer to a fixed concentration of sunitinib and monitoring changes in the chemical shifts of protons involved in the interaction (Athikomrattanakul et al. 2009). The data reported in Figure **1** confirm that Sunitinib interacts with all four functional monomers; its indole and methylidene groups make hydrophobic contacts with the aromatic system of 7-acryloyloxy-coumarin **5b**; the formation of hydrogen bonds between the indole NH proton and acceptors of N-acryloyl-tryptophan methyl ester **4b** and 4-vinyl pyridine **2b** is also observed; in addition the amide proton of sunitinib is also involved in hydrogen bonding to **4b**. The interactions with N-acryloyl-tyrosine methyl ester **2b** are weaker and involve mainly the amide group of sunitinib. The strongest interactions are observed with **5b** and **4b**, which appear to be the most promising monomers.

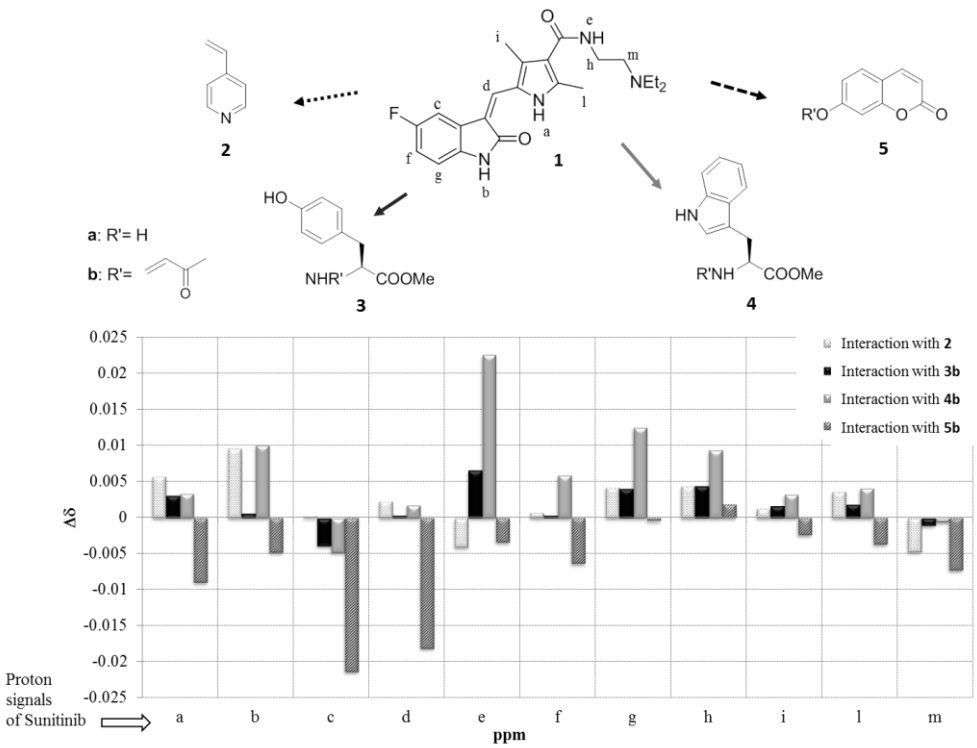

Figure 1 (new)

Synthesis and characterization of the polymers

Nanogels were synthesized by radical copolymerization of the four functional monomers **2b-5b** and acrylamide, with N,N'-ethylenebisacrylamide as the crosslinker, with a total monomer concentration (C_M) of 1%, in DMSO and AIBN as initiator as reported in Materials and Methods. The choice of acrylamide stemmed from the requirement of having polymeric matrices capable to easily dissolve as colloids in water. For the imprinted polymers, the template and the functional monomers, in a 1.2:1 molar ratio, were allowed to form the complex at 25°C for 40 min before polymerization (Pasetto et al. 2005). Eight nanogels were obtained by this method and their composition and characterisation are presented in **Table 1**. With the exception of NIP 0.2, which was poorly soluble, all nanogels showed good solubility and formed stable colloidal solutions in a 10% water : DMSO mixture. This solvent system appeared to be the most suitable and was used throughout for the characterisation. The particle size was evaluated by dynamic light scattering. The data are presented in **Table 1and figure S1** which shows a high degree of consistency with particle size by number all comprised

between 8 and 15 nm with good consistency. The results suggest that the polymers are mostly found as a fairly homogenous preparation, although the data for size by intensity does suggest the presence of a small fraction of aggregated nanoparticles, leading to the high intensity scattering around 130 nm diameter on average. However, this fraction was estimated to be less than 5% by volume analysis (Long et al. 2011). The particle size were also confirmed by transmission electronic microscopy, using graphene oxide grid, and the image for the coumarin-containing MIP 1.5 is shown in **Figure 2**.

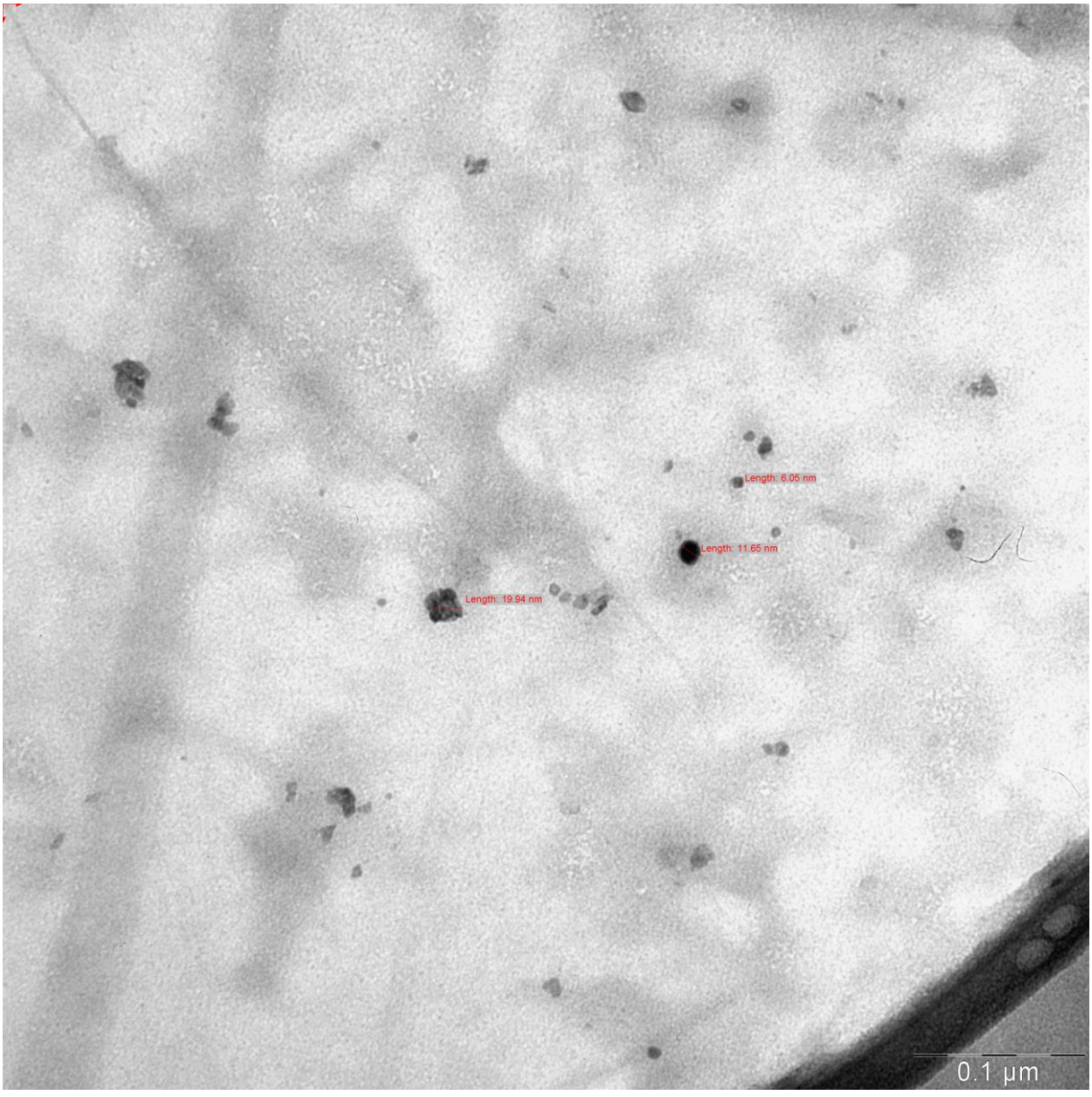

Figure 2 new

The coumarin containing polymers were characterized also by the content of the fluorescent tag incorporated, determined by UV, which showed interestingly some significant differences. The amount of bound coumarin in NIP **0.5** was found to be 550 pmol/μg, over twice the amount found in the imprinted material **1.5**, which contained 230 pmol/μg of the fluorescent label (**Table S2**, **Figure S2**). This would suggests that the formation of the template-monomer complex in the imprinted nanogels significantly impacts the incorporation of the coumarin unit. NMR experiments carried out with the coumarin monomer indicate that self-association of the monomer occurs at concentrations similar to those used during the nanogel synthesis (11 mM). This could explain the higher concentration of coumarin tag found in the non-imprinted polymer (**Figure S3**). The concentration of fluorescent tag in the different polymer preparations was taken into consideration when calculations of imprinting efficiency and rebinding were carried out.

Rebinding and selectivity

Rebinding tests were carried out by HPLC **(Table 1)**. The fluorescent MIP **1.5** is the best binder, capturing 35 nmol/mg of the target after several minutes, with good specificity, as indicated by the high value of the imprinting factor obtained. Although Sunitinib is always given in monotherapy without being co-administrated with other drugs, nevertheless the rebinding selectivity of MIP 1.5 was investigated using two common anticancer drugs : SN38 which has a similar shape and size as sunitinib, and paclitaxel, a much large molecule. Under the same experimental conditions the cross reactivity of MIP1.5 with SN38 and paclitaxel was found to be 23% and 3% respectively.

Fluorimetry

The presence of tyrosine, tryptophan and coumarin in the different nanogel preparations allows fluorimetric evaluation of the binding affinity at low drug concentrations. We have studied first the emission spectra of the fluorescent nanogels in their colloidal solutions in both DMSO and then in mixtures of DMSO and water, as these are the conditions in which the nanogels are

going to be applied. Characterisation techniques commonly used for bulk polymers or thin films could not be applied. The emission spectra for tyrosine and trypthopan containing nanogels are reported in the supplementary materials while the emission spectrum of MIP 1.5 is reported in **Figure 3a**. The emission of nanogels NIP 0.5 and MIP 1.5 is the highest, as expected given the high quantum yield of fluorescent tag. Monitoring of fluorescence over 30 hours provided evidence that the nanogels are photostable. Fluorescence quenching was indeed observed upon titration of all the polymeric nanogels with increasing concentrations of sunitinib. An example is reported in **Figure 3a** for MIP 1.5. The Stern-Volmer plots (Sarzehi and Chamani 2010) obtained with the tyrosine, tryptophan and coumarin MIPs show a bimodal quenching behaviour, with a first, higher slope, linear region at low concentrations of drug, and a second, lower slope, linear region at higher drug concentrations. Conversely, the Stern–Volmer plots reporting the fluorescence quenching of the free functional monomers upon titration with the drug show a single linear behaviour with a slope similar to the second region of the polymers **(Table 1, Figure 3b** for the coumarin derivatives, supplementary materials for the other compounds**)**.

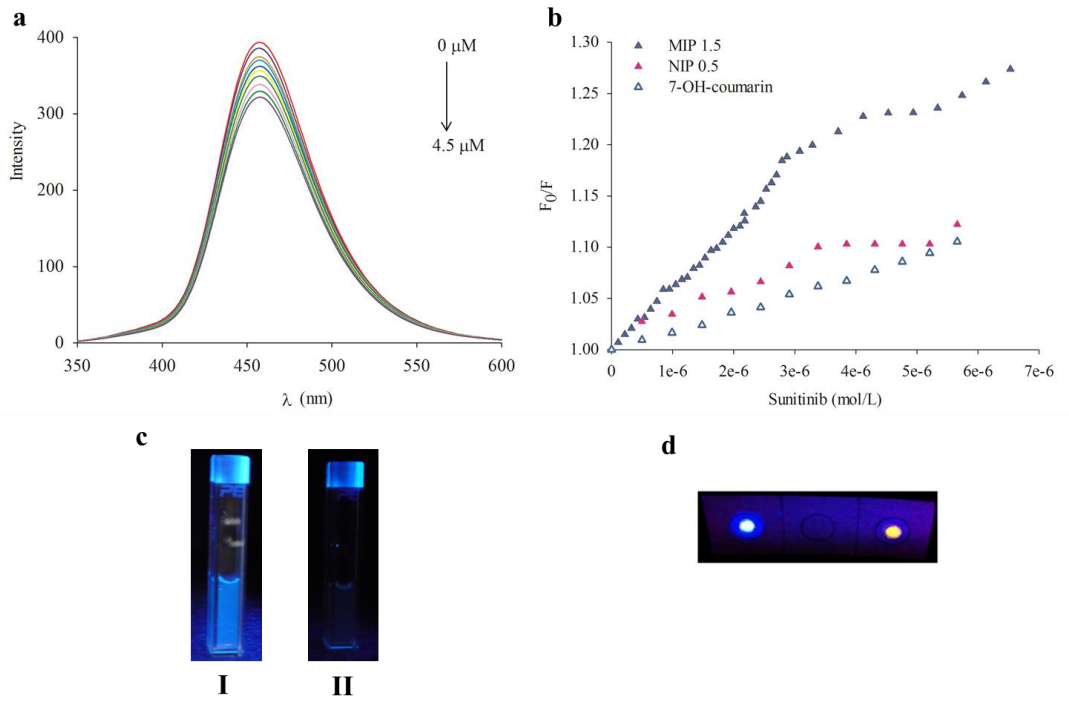

Figure 3 (new)

The efficiency of the drug in quenching the MIPs emission was investigated by the Stern-Volmer equation **1**(Gao et al. 2014), which was separately applied on the two linear regions of the Stern-Volmer plots.

$$F_0/F = K_{SV}^{app} \cdot [Q] + 1 \qquad \textbf{eq. 1}$$

.

The Stern–Volmer constants are reported in **Table 1**, together with the bimolecular quenching constants k_q^{app} calculated by equation **2**:

$$k_q^{app} = K_{SV}^{app} / \tau_0 \qquad \textbf{eq. 2}$$

where τ_0 is the lifetime of the fluorophores, which was assumed to be 4.3 ns for coumarin (Boens et al. 2007), 3.6 ns for tyrosine and 3.1 ns for tryptophan (Guzow et al. 2004; Szabo 1980). Even when the lower slope regions of the plots are included, k_q^{app} is larger than the limit value for the diffusion controlled quenching ($1 \cdot 10^{-10}$ $M^{-1}s^{-1}$). Thus, the observed quenching must be the consequence of a static interaction, *i.e.* the formation of a complex between the emitting polymers and the quencher drug ligand (Lakowicz 2006). The apparent Stern-Volmer constants

can therefore be regarded as apparent association constant for the MIPs-target complexes. The high Stern-Volmer constants measured at drug concentrations lower than 5 μM **(Table 1)** are most likely related to the presence of binding sites with a higher apparent binding affinity. Interestingly the concentration of such sites is very similar in all imprinted nanogels, suggesting that this is a feature likely to be related to the concentration of functional monomer and crosslinker used in the synthesis. Conversely, lower affinity binding sites on the polymer surface may be associated to the second region of the plots where the slope is similar to that obtained in the titration of the free functional monomers **(Table 1 and Figure 3b)**. The fluorescence quenching of polymer **1.5**, containing the coumarin unit, can be clearly visualised also by naked-eye **(Figure 3c** and **d)**.

Detection of sunitinib in plasma

MIP **1.5**, being the best binder and having excellent fluorescence properties, was chosen as the fluorescent nanogel to be used for the development of a direct assay for sunitinib in plasma samples.

Pre-treatment with a denaturing agent such as methanol or ethanol is generally required for the detection of drugs in plasma, where they are strongly associated to serum albumins. These common denaturing agents, however, cannot be used in this case, as the imprinted polymer releases the target drug when treated with alcohols. Thus, in this assay, DMSO has been used as denaturing agent. The action of DMSO on human plasma is very different from that of alcohol: the latter leads to the denaturation and precipitation of serum albumin, while DMSO leads to unfolding without precipitation (Sterling 2011, Tjernberg 2006). DMSO, however, is compatible with the imprinted polymer and we reasoned that serum albumin unfolding would be sufficient to release the albumin-bound drug. The designed assay thus requires simple dilution of the plasma sample in DMSO, addition of the fluorescent MIP and quantification of the fluorescence emission, which compared to a reference sample allows the quantification of the drug present in the plasma.

A calibration curve was initially obtained by titrating 60 μg/mL MIP **1.5** with increasing amounts of sunitinib in a 4:1 DMSO : water mixture (**Figure 4a**). The titration was repeated in triplicate experiments carried out with different polymer preparations and repeated in different days. The average calibration curve obtained from these titrations (**Figure 4a**, full circles) shows an excellent precision, with a within-run variability (CV) lower than 9%, and an average within-day variability lower than 5%. From the apparent Stern-Volmer constant for MIP**1.5** (**Table 1**) and the observed variability, a value of 400 nM can be obtained as the lower limit of detection of sunitinib, defined as the lowest concentration of sunitinib leading to an emission of polymer fluorescence that can be statistically differentiated from the reference (average emission under 3σ from the initial emission). As we have stated in the introduction there are no detection methods for sunitinib other than LC-MS. Clearly LC-MS is more sensitive than our system (which nevertheless is reported here as a non optimized proof of concept that could lead to more sensitive systems when exploited inside an optimized sensing device). However, our aim is to develop a system capable to detect plasma levels of sunitinib over the therapeutic range, and under this point of view, the sensitivity is satisfactory.

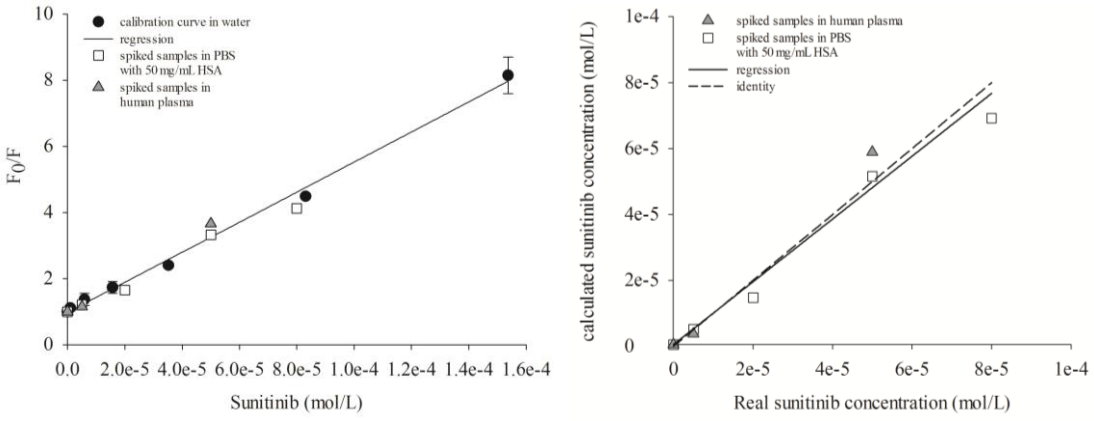

a **b**

Figure 4 (new)

Samples spiked with known quantities of sunitinib in both PBS and normal human plasma were treated with four volumes of DMSO to unfold proteins. In plasma, this treatment led to the formation of a small amount of white precipitate likely due to salts (as no absorbance at 280 nm was recorded after redissolving the precipitate in water). After centrifugation, MIP **1.5** was added from a mother solution in DMSO; the emission of the spiked samples was corrected for the emission of a plasma sample not containing sunitinib, and the drug concentration was calculated from the calibration curve obtained in 4:1 DMSO : water (**Figure 4**). The real and calculated concentrations of the drug in the spiked samples are reported in **Table 2**. Despite the samples were quantified using a calibration curve obtained in a different medium (DMSO : water), the accuracy was encouraging, and the calculated concentrations correlate well with the theoretical ones in both PBS and plasma solutions. The slope of the linear regression of these data is very close to the theoretical value of 1 for both the plasma samples and the buffer-albumin ones (**Figure 4b**). Therefore the robustness of the system upon changing the medium from DMSO : water to DMSO : PBS and DMSO : human plasma, is good.

4. Conclusions

In conclusion, we have designed and synthesized a set of fluorescent MIPS that bind sunitinib with good sensitivity. We have also developed a novel analytical protocol for the fluorimetric sensing of sunitinib in plasma samples exploiting the quenching of the MIP fluorescence by bound sunitinib. Simple dilution of human plasma with DMSO allows the detection of the drug with MIP **1.5**. The encouraging results obtained with this proof of concept open the way to the possible use of a fluorescent MIP as sensor for monitoring drug concentration directly in plasma with minimal sample treatment. We are currently working on portable fluorimetric systems based on this method, to be used as point of care devices.

Acknowledgements

We acknowledge the AIRC 5x1000 grant “Application of Advanced Nanotechnology in the Development of Innovative Cancer Diagnostics Tools”. We thank Dr G. Mastroianni for the TEM data.

5. References

Andriamanana, I., Gana, I., Duretz, B., Hulin, A., 2013. J. Chromotogr. B 926, 83-91.

Alnaim, L., 2007. J. Oncol. Pharm. Practice. 13, 207–221.

Altintas, Z., Guerreiro, A., Piletsky, S.A., Tothill, I.E., 2015. Sensors and Actuators B. 213, 305–313.

Athikomrattanakul, U., Katterle, M., Gajovic-Eichelmann, N., Sheller, F.W., 2009. Biosens. Bioelectron. 25, 82-87.

Awino, J.K., Zhao, Y., 2014. Chem. Commun. 50, 5752.

Bentolila, A., Vlodavsky, I., Ishai-Michaeli, R., Kovalchuk, O., Haloun, C., Domb, A.J., 2000. J. Med. Chem. 43, 2591-2600.

Blanchet, B., Saboureau, C., Benichou, A.S., Billemont, B., Taieb, F., Ropert, S., Dauphin, A., Goldwasser, F., Tod, M. 2009. Clin. Chim. Acta 404, 134-139.

Blanco-López, M.C., Lobo-Castañón, M.J., Miranda-Ordieres, A.J., Tuñón-Blanco, P., 2004. Trends in Analytical Chemistry. 23, 1.

Boens N., Qin W., Basaric´ N., Hofkens J., Ameloot M., 2007. Anal. Chem. 79, 2137-2149.

Carrasco, S., Benito-Peña, E., Walt, D.R., Moreno-Bondi, M.C., 2015. Chem. Sci. 6, 3139-3147.

De Bruijn, P., Sleijfer, S., Lam, M.H., Mathijssen, R.H.J., Wiemer, E.A.C., Loos, W.J., 2010. J. Pharm. Biomed. Anal. 51, 934-941

De Jonge, M.E., Huitema, A.D.R., Schellens, J.H.M., Rodenhuis, S., Beijnen, J.H., 2005. Clin Pharmacokinet. 44 (2), 147-173.

Etienne-Grimaldi, M.C., Renée, N., Izzedine, H., Gérard Milano, G., 2009 J. Chromatogr. B 877, 3757-3761

Faivre, S., Delbaldo, C., Vera, K., Robert, C., Lozahic, S., Lassau, N., Bello, C., Deprimo, S., Brega, N., Massimini, G., Armand, J.P., Scigalla, P., Raymond, E., 2006. J. Clini. Oncol. 24(1), 25-35.

Gao, L., Li, X., Zhang, Q., Dai, J., Wei, X., Song, Z., Yan, Y., Li, C., 2014. Food chemistry. 156, 1-6.

Guzow, K., Ganzynkowicz, R., Rzeska, A., Mrozek, J., Szabelski, M., Karolczak, J., Liwo, A., Wiczk, W., 2004. J. Phys. Chem. B. 108, 3879-3889.

Kollmannsberger, C., Bjarnason, G., Burnett, P., Creel, P., Davis, M., Dawson, N., Feldman, D.,

Lakowicz, J.R., 2006. Principles of Fluorescence Spectroscopy, Third Edition, Springer.

Long, Y., Philip, J.Y.N., Schillén, K., Liu, F., Ye, L., 2011. J. Mol. Recognit. 24, 619-630.

Luisi, I., Pavan, S., Fontanive, G., Tossi, A., Benedetti, F., Savoini, A., Maurizio, E., Sgarra, R., Sblattero, D., Berti, F., 2013. PLoS ONE. 8 (2), e56469.

Manju, S., Hari, P.R., Sreenivasan, K., 2010. Biosens. Bioelectron. 26, 894 – 897.

Moore, B.L., O'Reilly, R.K., 2012 J. Polym. Sci. A: polymer 50, 3567–3574.

Nezhadali, A., Senobari, S., Mojarrab, M., 2016. Talanta 146, 525-532.

Noble, M.E.M., Endicott, J.A., Johnson, L.N., 2004. Science. 303 (5665), 1800-1805.

Pasetto, P., Maddock, S.C., Resmini, M., 2005. Anal. Chim. Acta., 542, 66-75.

Prasad, B.B., Kumar, D., Madhuri, R., Tiwari, M.P., 2012. Electrochim. Acta. 71, 106-115.

Prasad, B.B., Srivastava, S., Tiwari, K., Sharma, S.P., 2009. Sens. Mat. 21 (6), 291-306.

Sinkel, C., Greiner, A., Agarwal, S., 2010 Macromol. Chem. Phys. 211, 1857–1867.

Sterling, H.J., Prell, J. S., Cassou, C. A., Williams, E. R., 2011. J. Am. Soc. Mass Spectrom. 22, 1178-1186.

Thibert, V., Leageay, P., Chapuis-Hugon, F., Pichon, V., 2014. J. Chromatogr. B. 949-950, 16-23.

Tjernberg, A., Markova, N., Griffiths, W. J., Hallen D., 2006. J. Biomol. Screen. 11 (2), 131-137.

Ton, X.A., Bui, B.T.S., Resmini, M., Bonomi, P., Dika, I., Soppera, O., Haupt, K., 2013. Angew. Chem. Int. Ed. Engl**.** 52 (32), 8317-8321.

Walko, C.M, McLeod, H.L., 2014. J. Clin. Oncol., 32 (24), 2581-2586

Wei, F., Wu, Y., Xu, G., Gao, Y., Yang, J., Liu, L., Zhou, P., Hu, Q., 2014. Analyst DOI: 10.1039/c4an00951g

Yang Y., Yu J., Yin J., Shao B., Zhang, J., 2014. J. Agric. Food Chem. 62, 11130−11137.

Zhang, J., Yang, P.L., Gray N.S., 2009. Nature Rev. Canc. 9 (1), 28-39.

Szabo A.G., Rayner, D.M ., 1980. J.Am.Chem.Soc, 102, 2.

Sarzehi, S., Chamani, J., 2010. Int. J. Biol. Macromol. 47, 558–569.

Tables

Table 1: physical and binding properties of the MIPs. [1]DLS size number measured in a 10% water:DMSO mixture on 250 μg/mL colloidal solutions of nanogels (NIP 0.2 was dissolved in DMSO only due to its poor solubility in the water mixture. [2]Rebinding measured by HPLC on a 50 μM solution containing 1 mg/mL polymer. [3]Apparent Stern-Volmer constant measured at ligand concentrations *below* and (*above*) 5μM. The Stern-Volmer constants measured for the interactions of **1** with fluorophores **3a**, **4a** and **5a** were 12.7, 12.2 and 18.4 respectively. [4]Apparent quenching constants measured at ligand concentrations *below* and (*above*) 5μM. The quenching constants measured for the interactions of **1** with fluorophores **3a**, **4a** and **5a** were 3.5, 3.9 and 4.3 respectively.

Nanogel	**Functional monomer**	**Crosslinker (%)**	**DLS Size *Number*[1] (nm) AVG**	**PDI**	**Rebinding[2] nmol mg^{-1}**	**IF**	**K_{sv}[3] 10^3Lmol^{-1}**	**k_q[4] 10^{12}Lmol^{-1} s^{-1}**
MIPs								
1.2	2	70	8.10±2.5	0.65	19	6	-	-
1.3	3b	70	11.6±2.5	1	14	3	*37.6* (14.4)	*10.4* (4.0)
1.4	4b	70	11.9±3.7	0.35	20	3	*25.2* (10.7)	*8.1* (3.5)
1.5	5b	70	12.5±3.3	0.50	42	6	*61.0* (15.5)	*14.2* (3.6)
NIPs								
0.2	2	70	203±25	1	3			
0.3	3b	70	10.5±2.0	0.25	4			
0.4	4b	70	14.7±4.1	0.51	6			
0.5	5b	70	13.7±4.1	0.54	7		*26.5* (8.2)	*6.2* (1.9)

Table 2: Real and calculated sunitinib concentrations in spiked samples

Real sunitinib concentration [10^{-6} mol·L^{-1}]	**Calculated sunitinib concentration [10^{-6} mol·L^{-1}]**	
	In PBS with 50 mg·mL^{-1} HSA	**In plasma**
5	5.12	3.75
20	14.7	-
50	51.6	58.9
80	69.2	-

Captions to Figures

Figure 1: Structures of sunitinib and of functional monomers; changes in the chemical shifts of selected protons of the target drug upon addition of the functional monomers (at a 1:14 molar ratio). The titrations were carried out in DMSO-d_6 at room temperature.

Figure 2: TEM image of MIP 1.5 over a graphene oxide grid

Figure 3: a) Emission spectrum of MIP 1.5 (60 μg/mL) alone and upon addition of increasing concentrations of sunitinib. b) Stern-Volmer plots of the emissions of MIP **1.5**, NIP **0.5** and 7-hydroxycoumarin upon addition of increasing concentrations of sunitinib. cI) picture of a 60 μg/mL solution of MIP 1.5 upon excitation with a 365 nm UV lamp. cII) picture of the same solution after addition of 50 μM sunitinib; d) Picture of a spot of 25 μg MIP 1.5 on filter paper before and after the addition of 300 ng of sunitinib.

Figure 4: a) distribution of the spiked samples in PBS with 50 mg/mL HSA and in human plasma on the calibration curve; b) correlation between the calculated sunitinib concentration and the real drug concentration of spiked samples in PBS with 50 mg/mL HSA and in plasma; dotted line: identity; full line: regression.